Available online at www.sciencedirect.com
ScienceDirect
Catalysis Today 136 (2008) 121–127
CATALYSIS TODAY
www.elsevier.com/locate/cattod

NO_x uptake on alkaline earth oxides (BaO, MgO, CaO and SrO) supported on γ-Al_2O_3

Christelle Verrier, Ja Hun Kwak, Do Heui Kim, Charles H.F. Peden, János Szanyi *

Institute for Interfacial Catalysis, Pacific Northwest National Laboratory, P.O. Box 999, MSIN: K8-80, Richland, WA 99352, USA

Available online 21 February 2008

Abstract

NO_x uptake experiments were performed on a series of alkaline earth oxide (AEO) (MgO, CaO, SrO, BaO) on γ-alumina materials. Temperature programmed desorption (TPD) conducted in He flow revealed the presence of two kinds of nitrate species: i.e. bulk and surface nitrates. The ratio of these two types of nitrate species strongly depends on the nature of the alkaline earth oxide. The amount of bulk nitrate species increases with the basicity of the alkaline earth oxide. This conclusion was supported by the results of infrared and ^{15}N solid-state NMR studies of NO_2 adsorption. Due to the low melting point of the precursor used for the preparation of MgO/γ-Al_2O_3 material ($Mg(NO_3)_2$), a significant amount of Mg was lost during sample activation (high temperature annealing) resulting in a material with properties very similar to that of the γ-Al_2O_3 support. The effect of water on the NO_x species formed in the exposure of the AEO-s to NO_2 was also investigated. In agreement with our previous findings for the BaO/γ-Al_2O_3 system, an increase of the bulk nitrate species and the simultaneous decrease of the surface nitrate phase were observed for all of these materials.
Published by Elsevier B.V.

Keywords: NO_x storage; Basicity; BaO/γ-Al_2O_3; MgO/γ-Al_2O_3; SrO/γ-Al_2O_3; CaO/γ-Al_2O_3; NO_2 TPD; FTIR; ^{15}N s.s. MAS NMR

1. Introduction

Lean NO_x trap systems (LNTs) have been considered as one of the most promising solutions for exhaust emission control in diesel engine applications [1–3]. Typical LNT catalysts consist of three principal components: precious metal (PM) (1–2 wt% of Pt and/or Rh), a storage material (10–20 wt% of alkaline earth oxide), and a high surface area support material (in most cases γ-alumina). There is a general agreement that the process of NO_x uptake involves the oxidation of NO to NO_2 in the presence of oxygen over PM sites [4–6], followed by the storage of NO_2 on the alkaline earth oxide as nitrites and nitrates during long lean (oxygen rich) periods. These strongly-bound NO_x species are then reduced by reductants over the PM to N_2 during a subsequent, short fuel rich period. As the performances of these catalysts strongly depend on the storage capability, it is very important to better understand the interactions between various NO_x species with different alkaline earth oxides. Many experiments have evidenced that the presence of BaO in LNT materials strongly enhances NO_x storage [7–13]. Two types of Ba-nitrate species have been identified on this catalyst: surface and bulk nitrate species that exhibit distinctively different thermal and spectroscopic characteristics [11].

Studies discussing the NO_x storage properties of alkaline earth oxides other than BaO are scarce [14]. In order to be able to choose the proper base material (AEO) for this particular application, it is imperative to conduct studies that compare the properties of these materials. It is also important to compare the NO_x storage properties of these systems at identical AEO loadings. Previous studies by our group have shown the effect of Ba loading on NO_x storage [10,11,15]. The optimal NO_x storage properties were found at BaO loadings of around 20% BaO/γ-Al_2O_3. Based on these results, a series of AEO-loaded alumina samples was prepared with AEO molar loadings corresponding to that of the 20 wt% BaO/γ-Al_2O_3. In the present study, we used FTIR spectroscopy, ^{15}N solid-state MAS NMR and TPD experiments to compare the NO_x storage properties of five different materials: γ-Al_2O_3, CaO/γ-Al_2O_3, BaO/γ-Al_2O_3, SrO/γ-Al_2O_3 and MgO/γ-Al_2O_3.

* Corresponding author. Tel.: +1 509 371 6524; fax: +1 509 371 6498.
E-mail address: janos.szanyi@pnl.gov (J. Szanyi).

0920-5861/$ – see front matter. Published by Elsevier B.V.
doi:10.1016/j.cattod.2007.12.138

2. Experimental

The NO_x storage materials used in this study were prepared by an incipient wetness method, in accord with our previously published preparation procedure for $BaO/\gamma\text{-}Al_2O_3$ [15]. Specifically, an aqueous $Ba(NO_3)_2$ solution (Aldrich) was used to yield 20 wt% of BaO on a 200 m^2/g $\gamma\text{-}Al_2O_3$ support (Condea). For the preparation of other NO_x storage materials, the relevant alkaline earth nitrate solutions were used to reach the same AEO molar loading (33%) as we did for BaO. After impregnation, the materials were dried at 393 K and then the nitrates were converted to oxides by calcination at 773 K in a 20% O_2 in N_2 flow for 2 h.

The NO_2 adsorption studies were carried out in a fixed bed quartz reactor under continuous flow. The materials (0.1 g) were first saturated with NO_2 at 300 K using a 100 cc/min 0.5% NO_2/He gas mixture (99.999% purity, Matheson). After saturation, the catalysts were purged under He flow for 1 h at 300 K. Finally, the reactor temperature was raised in a temperature programmed fashion at 8 K/min to 973 K, the evolution of NO_x species were monitored with a chemiluminescence NO_x analyzer (42C, Thermo Environmental). The concentrations of total NO_x and NO were determined simultaneously, and the amount of NO_2 released is then deduced as the difference between $NO_x - NO$ ($[NO_2] = [NO_x] - [NO]$). TPD experiments in the presence of water in the He flow were also carried out. Since some weakly-held NO_x (e.g. N_2O_3) species were also formed on the catalyst surface during the adsorption at 300 K, in these experiments the NO_2 uptake was conducted at 523 K in order to avoid the formation of these weakly-held NO_x species and their interaction with water. The materials were then cooled down to 393 K and the TPD experiment was run in a 1% H_2O/He flow. FTIR spectroscopy measurements to characterize the NO_x species on these $AEO/\gamma\text{-}Al_2O_3$ materials were carried out using a Nicolet Magna-IR 750 spectrometer operating at 4 cm^{-1} resolution. Prior to each spectral series acquisition, a background scan was acquired on the clean, adsorbate free sample. The infrared cell was a $2^3/_4$ in. six-way stainless steel cube equipped with CaF_2 windows. The cell is connected to a gas handling/pumping station and through both leak and gate valves to a mass spectrometer (UTI 100C). The catalyst sample was pressed onto a fine tungsten mesh, which is mounted onto a copper sample holder. Prior to each experiment, the catalyst was first pre-heated at 973 K in vacuum to eliminate residual species on the surface. The clean samples were exposed to small aliquots of NO_2 at 300 K until no change in the IR spectra was seen (i.e. until saturation). Subsequently, the cell was evacuated, and the sample temperature was raised at a constant rate of 12 K/min while the desorbing species were monitored via a mass spectrometer (UTI 100C).

^{15}N solid-state NMR spectra were acquired on a Varian/Chemagnetics CMX Infinity 300 MHz instrument, equipped with a Varian/Chemagnetics 7.5 mm HX MAS probe operating at a spectral frequency of 30.40651 MHz. In the in-situ NMR cell, 0.5 g of $AEO/\gamma\text{-}Al_2O_3$ samples (pre-calcined at 773 K for 2 h in air) were pretreated under vacuum ($<1 \times 10^{-7}$ Torr) at 773 K for 2 h in order to remove adsorbed water. After dehydration, the samples were cooled down to room temperature for NO_2 adsorption. The amount of NO_2 adsorbed was kept around 5–10 Torr equilibrium pressure. The NO_2-saturated samples were transferred into the gas-tight rotor (7.5 mm O.D.) for solid-state ^{15}N NMR measurements. All ^{15}N s.s. MAS NMR spectra were externally referenced to ^{15}N-ammonium chloride at 0 ppm. All spectra were obtained applying 10 s recycle delay and 5 kHz spinning.

3. Results and discussion

3.1. TPD

Fig. 1 shows the results of TPD experiments conducted under He flow on each NO_2-saturated (at 300 K) sample. Panel (A) of Fig. 1 displays the evolution of NO_2 as a function of temperature for the alkaline earth oxides studied (the results for the alumina support are shown as a reference as well). A systematic increase in the temperature of maximum NO_2 desorption rate can clearly be seen from the lowest value for $MgO/\gamma\text{-}Al_2O_3$ (~675 K) (same as that of the alumina support), followed by the $CaO/\gamma\text{-}Al_2O_3$ (690 K), to the highest ones for BaO- and $SrO/\gamma\text{-}Al_2O_3$, which were identical within the accuracy of the measurement (~705 K). The basicity of the surface seems to govern the decomposition temperature of these surface nitrate species. The more basic is the adsorbent,

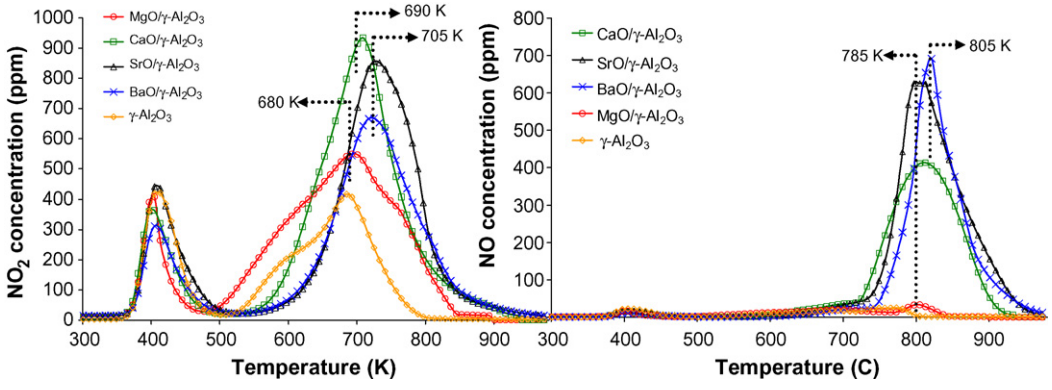

Fig. 1. TPD spectra from BaO-, SrO-, CaO- and $MgO/\gamma\text{-}Al_2O_3$ after NO_2 saturation at 300 K: NO_2 release (A) and NO release (B) (heating rate: 8 K/min).

Table 1
Summary of the amount of NO_2 and NO released during TPD after NO_2 saturation at 300 K on BaO-, SrO-, CaO- and MgO/γ-Al_2O_3

	MgO/Al_2O_3	CaO/Al_2O_3	SrO/Al_2O_3	BaO/Al_2O_3
NO_2 (%)	94.2	53.3	45.4	36.4
NO (%)	5.8	46.7	54.6	63.6
NO_2 (mol/mol AEO)	0.29	0.19	0.22	0.16
NO (mol/mol AEO)	0.02	0.17	0.26	0.28
NO_x (mol/mol AEO)	0.31	0.36	0.48	0.44

the stronger the bonding to the surface, and, therefore, the higher the temperature where adsorbed NO_2 is released [16]. The corresponding TPD profiles of NO evolution are shown in panel (B) of Fig. 1 for each alkaline earth oxide. The temperature of maximum NO desorption rate for these materials fall into the very narrow range of 785–805 K, with no clear change going from MgO to BaO (although the temperature of maximum desorption rate was the lowest for MgO, and the highest for BaO). The amount of NO and NO_2 released from the four AEO/γ-Al_2O_3 storage materials, estimated from the integrated intensities under the NO_2 and NO desorption profiles above 475 K, are summarized in Table 1. The percentages shown are normalized values, as the total integrated intensities between 475 and 970 K temperature interval (both NO_2 and NO desorption features) were chosen as 100% for each AEO/γ-alumina sample. The amount of NO_2 released, as a percentage of the total NO_x desorbed, sharply decreases from MgO to SrO, while for BaO it is very similar to that observed for SrO. On the other hand, the normalized amount of NO released (NO %) is systematically decreasing in the order of $BaO \geq SrO > CaO > MgO \sim \gamma\text{-}Al_2O_3$. The amount of NO released from MgO/γ-Al_2O_3 is very small (almost non-existent, very similarly to NO desorption from γ-Al_2O_3), while that for the BaO/γ-Al_2O_3 and SrO/γ-Al_2O_3 systems are almost identical. The presence of a small NO_2 desorption peak at a lower temperature around 393 K can also be seen for all four samples. This feature has been attributed [15] to the desorption of weakly-held NO_2 and/or the decomposition of weakly adsorbed N_2O_3 species formed in the $NO + NO_2$ reaction, and adsorbed on the Al_2O_3 support. This assignment has been supported by the results of IR spectroscopy measurements following NO_2 exposure of these supported AEO samples (discussed in Section 3.2).

Evidence for the presence of two different types of nitrate species on NO_2-saturated BaO/γ-Al_2O_3 samples has been reported in previous studies from our group [5,7,10,11] and other laboratories [13,17]. Over the 20% BaO/γ-Al_2O_3 sample the formation of both surface and bulk nitrate species were evidenced. These two nitrate species have been shown to have distinctive spectroscopic signatures (both IR and NMR) that allow their identification. Work by Szanyi et al. has also revealed the variation in the ratio of different nitrate species as a function of BaO loading. While the surface to bulk nitrate ratio was larger than one for the 8 wt% BaO/γ-Al_2O_3 sample, that was smaller for the 20 wt% one. The formation of large $Ba(NO_3)_2$ crystallites was also evidenced as the sample temperature was raised in the presence of NO_2, underscoring the significant morphology changes that can occur in these materials [11].

The results of previous studies on BaO/γ-Al_2O_3 NO_x storage materials have shown that surface nitrates decompose first, releasing NO_2 only, while bulk nitrates decompose at higher temperature with the release of both NO and O_2. Similarly to the BaO/γ-Al_2O_3 material, we propose that for all the AEO/γ-Al_2O_3 samples studied here the NO_2 peak in the TPD spectra (lower temperature desorption feature) originates from the decomposition of surface alkaline earth nitrate species, and the second desorption feature (NO) (higher temperature desorption peak) is related to the decomposition of bulk alkaline earth nitrates. The results summarized in Table 1 show that the decrease in the amount of NO_2 released correlates with the presence of a lower amount of surface nitrates species. At the same time, the increase in the amount of NO released corresponds to the increase of the amount of bulk nitrate species. In the series of the AEO/γ-Al_2O_3 materials the amount of bulk nitrate species increase from MgO/γ-Al_2O_3 (that is negligible) to CaO/γ-Al_2O_3, and finally SrO/γ-Al_2O_3 and BaO/γ-Al_2O_3, that have the highest amount. Concomitantly, an opposite trend is observed for the surface nitrate species along the series. These results suggest that with increasing basicity of the AEO the amount of bulk nitrates increases (at least when the oxides are supported on γ-Al_2O_3). The increasing decomposition temperature of bulk nitrates are in line with the bulk decomposition temperatures of the unsupported alkaline earth nitrates ($Ca(NO_3)_2$: 835 K; $Sr(NO_3)_2$: 845 K and $Ba(NO_3)_2$: 850 K).

In order to be able to compare the NO_x uptake efficiencies of these AEO/alumina storage materials on a more quantitative manner we contacted chemical analysis to precisely determine the amount of AEO present after sample activation (i.e. after calcination at 775 K). Based on the results of these chemical analysis we determined the amounts of NO and NO_2 evolved during the TPD experiment as mole per mole of alkaline earth oxide present. These results confirm that the NO_2 uptake increased as the basicity of the AEO increased ($MgO < CaO < SrO \sim BaO$). Furthermore, it also showed that the NO_2 uptake efficiencies of SrO and BaO are practically identical, and that of SrO might even be better than BaO (although the difference between these two oxides are well within the accuracy of these measurements). The TPD profiles of Fig. 1 also indicate that the alumina support itself has a significant capacity for NO_2 uptake, as it forms surface nitrates exclusively. Comparing the TPD traces of γ-Al_2O_3 and MgO/γ-Al_2O_3 reveals striking similarities. This can easily be explained by the results of the chemical analysis that showed a ~50% loss of Mg from the support during sample activation. It is also evident from these TPD curves that the amount of NO_2 released was thus overestimated for the MgO/γ-Al_2O_3 sample, since a large fraction of the NO_2 uptake was associated with the alumina support itself. Interaction of NO_2 with the AEO-free alumina surface may also influence the calculated amounts of NO_2 desorbed in the case of the other AEO/γ-alumina samples. However, as we have seen for the 20 wt% BaO/γ-Al_2O_3 case this contribution is fairly small [11].

3.2. FTIR Spectroscopy

FTIR spectroscopy was used to identify the NO_x species formed on the series of AEO/γ-Al_2O_3 NO_x storage materials upon NO_2 adsorption at 300 K. As we have shown in detail for the 20 wt% BaO/γ-Al_2O_3 storage material [18], both nitrites (1222 cm^{-1}) and nitrates (1310, 1440, and 1577 cm^{-1}) formed on the clean, activated sample upon its initial exposure to NO_2 at 300 K. After prolonged exposure to NO_2 the nitrites were converted to nitrates, and both surface (1310 and 1577 cm^{-1}) and bulk (1320 and 1440 cm^{-1}) nitrates formed. Fig. 2 presents the infrared results obtained after NO_2 exposure and subsequent evacuation of the activated NO_x storage materials at 300 K. After the initial adsorption of small doses of NO_2 on every alkaline earth oxide, the infrared spectrum of each material shows bands that we can attribute to both nitrite and nitrate species (not shown). At higher doses of NO_2, the intensities of vibrational features characteristic of different types of nitrate species (surface and bulk) are observed, while those of the nitrites disappear. On γ-Al_2O_3 the NO_x species we observe are exclusively surface nitrates coordinated to the γ-Al_2O_3, as it has been discussed in detail by Grassian and co-workers [19] and by us [20]. For the MgO/γ-Al_2O_3 sample, increases in the intensities of all the NO_x-related IR features are observed, although the positions of the IR features from this material following NO_2 exposure are very similar to those seen from the pure alumina support. This can be associated with the presence of only a small amount of MgO on the γ-Al_2O_3 surface. The addition of the other AEO-s to the γ-Al_2O_3 support results in the decrease, and almost complete disappearance of the alumina surface-related nitrate bands. In these samples the presence of both surface and bulk nitrates of the AEO can clearly be seen, together with the small shoulders at 1250 and 1630 cm^{-1}, indicating that surface nitrates are formed on the AEO-free alumina support as well. The IR features characteristic of surface and bulk nitrate species of AEO-s develop in a similar fashion as we have previously shown for the BaO/γ-Al_2O_3 system [11]. The splitting of the ν_3 vibrations of both surface and bulk nitrates result in two sets of IR features for each AEO. For BaO/γ-Al_2O_3, at the high BaO coverage used for this sample (20 wt%), the low wavenumber components of these two vibrations overlap so strongly that they cannot be distinguished (band at 1310 cm^{-1}). For the other AEOs the low wavenumber components of the ν_3 vibrations of the surface and bulk nitrates can clearly be distinguished. The position of the low frequency component of this vibration of the surface nitrate feature gradually shifts from 1260 cm^{-1} for MgO, 1280 cm^{-1} for CaO, 1287 cm^{-1} for SrO, to 1310 cm^{-1} for BaO (gradual blue shift). On the other hand, the high frequency component of this vibration shifts to lower wavenumbers, going from MgO to BaO (red shift) (1593 cm^{-1}, 1582 cm^{-1}, 1580 cm^{-1} and 1577 cm^{-1}). There are systematic shifts in the frequencies of the ν_3 vibrational features of the bulk AEO-nitrates as well. The low frequency component gradually red shifts from 1328 cm^{-1} for CaO, to 1322 cm^{-1} for SrO, and finally to 1320 cm^{-1} for BaO, and the high frequency one red shifts as well (1480 cm^{-1}, 1463 cm^{-1} and 1440 cm^{-1}). Both the low and high frequency components of the ν_3 vibration of the bulk nitrate ions gradually red shift, although the extent of the shift is more pronounced for the high frequency component. This results in a systematic decrease in the frequency difference ($\Delta\nu_3$) between these two features: 152 cm^{-1} for CaO, 140 cm^{-1} for SrO and 120 cm^{-1} for BaO. Frequency shifts, similar what we observed here, have been reported in a combined IR and Raman spectroscopy study of crystalline AE-nitrates (CaO, SrO and BaO) [21]. They attributed the observed shifts primarily to the structural differences in the crystals due to the variations in the radii of the AE ions. In our view, the additional factor influencing the observed frequency shifts is the difference in the basicity of the AEO, that is correlated to their cationic sizes as well. Besides the frequency shifts of the nitrate vibrations, the relative intensities of the surface and bulk nitrates seem to change systematically as well. With the increase in the basicity of the AEO, the relative intensities of the bulk nitrate features increase at the expense of the surface nitrates.

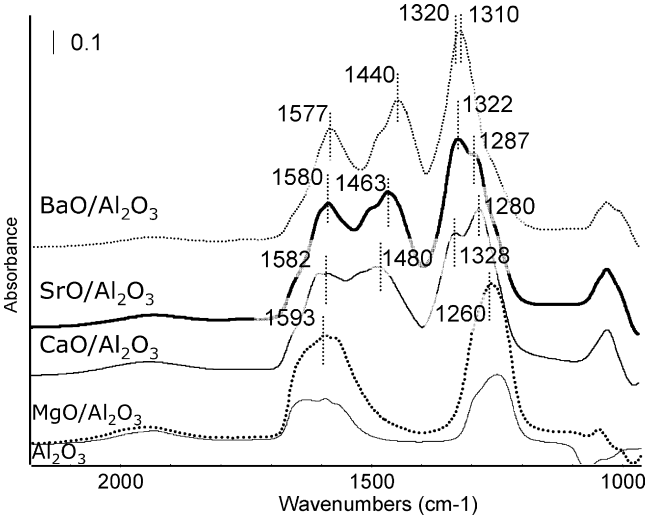

Fig. 2. Comparison of infrared spectra from γ-Al_2O_3 and alkaline earth oxides supported on alumina (BaO/γ-Al_2O_3, SrO/γ-Al_2O_3, CaO/γ-Al_2O_3 and MgO/γ-Al_2O_3) after NO_2 saturation and evacuation under high vacuum at 300 K.

These results are consistent with the ones obtained in the TPD experiments: both surface and bulk nitrates are present in the NO_2-saturated AEO/γ-Al_2O_3 materials (except MgO, in which only surface nitrates were seen), and the amount of bulk nitrates formed increases as the basicity of the AEO increases (CaO < SrO < BaO).

In the IR spectra collected after room temperature NO_2 saturation of all the samples studies here we can clearly observe a broad absorption feature in the 1920–1960 cm^{-1} region. This IR band has been previously assigned to N_2O_3 adsorbed onto the alumina support [19,20], and may have some contribution from the NO^+ species that can be formed by the disproportionation of NO_2 [20].

3.3. ^{15}N solid-state MAS NMR

^{15}N solid-state MAS NMR spectra obtained from the γ-Al_2O_3, and AEO (MgO, CaO, SrO, and BaO)/γ-Al_2O_3 materials following $^{15}NO_2$ saturation at room temperature

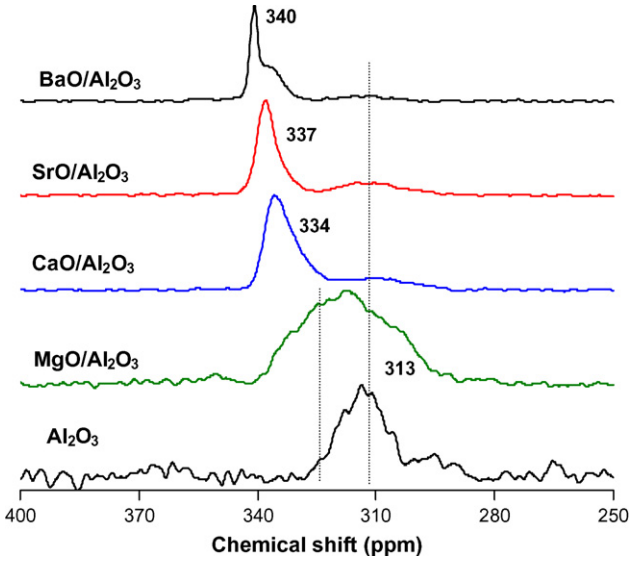

Fig. 3. ^{15}N solid-state MAS NMR spectra of γ-Al_2O_3, and alkaline earth oxides (MgO, CaO, SrO, BaO) supported on γ-alumina after NO_2 saturation at 300 K.

are displayed in Fig. 3. On the γ-Al_2O_3 support, a broad NMR feature centered at 313 ppm chemical shift (relative to the $^{15}NH_4Cl$) is seen. This peak has been assigned to the ^{15}N atoms in the surface nitrate species of the alumina support [11]. For MgO/γ-Al_2O_3 a very broad NMR feature is recorded that may be resolved into two highly overlapping bands at 313 and ~325 ppm. On the other three AEO/γ-Al_2O_3 systems two overlapping NMR bands are observed. These two peaks are best resolved in the case of BaO/γ-Al_2O_3, and have been assigned to ^{15}N in bulk (340 ppm) and surface (335 ppm) nitrates. In addition to the high extent of overlap of the NMR features representing the two different types of AEO-related nitrates, a small, but systematic shift to lower chemical shifts is observed going from BaO to CaO. For SrO/γ-Al_2O_3 the peak is centered at 337 ppm, while for CaO it is at 334 ppm.

As the results of all the experiments (TPD, FTIR, NMR) discussed so far indicate, MgO has a particular behavior: the amount of bulk nitrate phase is non-existent, and all the spectroscopy data suggest that this sample is very similar to the AEO-free alumina support material. The seemingly out-of-trend behavior of MgO/γ-Al_2O_3 may be explained by the precursor ($Mg(NO_3)_2$) used for preparation of this material. We have chosen the nitrate salts for all the AEO/γ-Al_2O_3 preparations in order to avoid the carbonate formation associated with other commonly used precursors (e.g. acetates). However, $Mg(NO_3)_2$, in comparison to the other AE-nitrates, has an unusually low melting point of ~373 K. Therefore, it is highly probable that during sample activation (annealing at 773 K) at temperatures above the melting point most of the $Mg(NO_3)_2$ evaporates prior to its decomposition. In fact, the results of chemical analysis have confirmed that about 50% of the Mg precipitated onto the γ-alumina support was missing from the 773 K annealed $Mg(NO_3)_2$/γ-Al_2O_3 sample. This means that the actual loading of MgO on this storage material is about 4.75 wt% instead of 9.45 wt%. This loss of Mg during sample activation would explain why all the data obtained from this material resemble that collected from γ-Al_2O_3. The small amount of MgO present on the alumina support is in the form of very well dispersed surface MgO, similar to that we have observed for BaO at low coverage over a γ-Al_2O_3 support [22]. The complete absence of spectroscopic features characteristic of bulk $Mg(NO_3)_2$ can now be understood.

3.4. The effect of water on the NO_x species in NO_2-saturated AEO/γ-Al_2O_3

The effect of water on the NO_x species stored on the AEO/γ-Al_2O_3 materials was studied last. To this end we conducted two sets of experiments in order to follow the changes in the nature of the NO_x species (IR), and those in their thermal decomposition properties (TPD). In the IR cell the activated samples were first saturated with NO_2, the excess NO_x was then evacuated, and finally these NO_x/AEO/γ-Al_2O_3 samples were exposed to 1 Torr of H_2O, followed by evacuation at 300 K. Fig. 4 summarizes the infrared data for all samples studied and

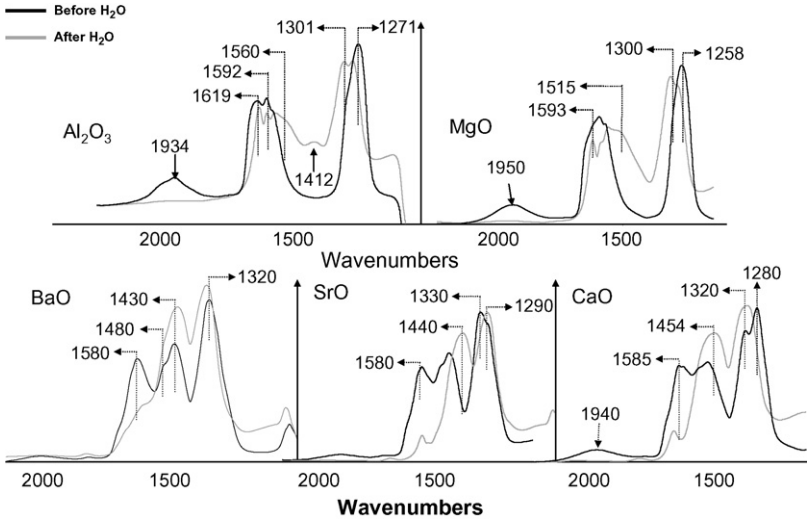

Fig. 4. Infrared spectra after NO_2 adsorption and evacuation, followed by water adsorption and evacuation on BaO-, SrO-, CaO- and MgO/γ-Al_2O_3 at 300 K.

obtained at room temperature after evacuation. The black spectrum in each panel was recorded after NO_2 saturation and evacuation, while the grey ones were obtained after these NO_2-saturated samples were exposed to water. Similarly to the results discussed above for the dry samples, the data obtained after water exposure show two distinct trends: on one side the NO_2-saturated alumina and MgO/γ-Al_2O_3 samples behaved identically, while the other three AEO-s exhibited similar trends. In the case of the alumina support and the MgO/γ-Al_2O_3 the changes seem to correspond to the changes in the surface nitrate coordination geometry on γ-Al_2O_3 as a result of H_2O adsorption. As we have discussed it in detail elsewhere [23,24], the exposure of NO_2-saturated γ-Al_2O_3 to H_2O did not affect the amount of strongly-held NO_x species; however, it significantly influenced the coordination of nitrate species. Specifically, the bridge-bound nitrates converted to monodentate ones. The changes in the IR spectra of the other NO_2-saturated AEO/γ-Al_2O_3 samples are very similar to each other. In all three cases the intensities of the surface nitrate-related IR bands (∼1580 cm^{-1} and ∼1280–1320 cm^{-1}) decreased, while those of the bulk nitrates (located between 1430 and 1460 cm^{-1} and around 1300 cm^{-1}) increased.

Fig. 5 shows the results of the TPD experiments conducted under a flow of 1% water in He following NO_2 saturation (at 523 K) for all samples studied (panel A shows the NO_2 trace, and panel B the NO trace). In accordance with the IR results, the amount of NO_2 released (which is characteristic of the decomposition of surface nitrates) decreases from γ-Al_2O_3 (and MgO/γ-Al_2O_3) to BaO/γ-Al_2O_3 and, concomitantly, the amount of NO increased along the series. Most importantly, the NO_2 to NO ratio in the TPD changed as well. The more basic the AEO the more significant the conversion of the surface nitrates to bulk nitrates. Table 2 gives a comparison of the amount of NO and NO_2 released for each NO_x storage material during the TPD, with and without water. Again, the percentages of NO_2 and NO released are shown in this table are normalized to the total amount of NO_x desorbed above 473 K.

The effect of water in the carrier gas during a TPD experiment on the desorption profiles of NO_2 and NO on NO_2-saturated BaO/γ-Al_2O_3 has been observed by Cant and Patterson [25]. Similarly to the changes in the NO_2 and NO peak intensities we have discussed above, they also observed a shift to higher temperature in the maximum NO_2 desorption rate. Their preferred explanation for these observations was the formation of a $Ba(OH)_2$ crust on the decomposing particles in the presence of water that slowed down the diffusion of the NO_x species to the surface. As we have suggested previously for the BaO/γ-Al_2O_3 system [26], these changes were probably the consequence of the morphology changes in the presence of water. We have also shown for the BaO/γ-Al_2O_3 case that the effect of water was completely reversible; i.e. when water was removed from the IR cell (by evacuation) and from the sample surface (by heating) some of the bulk nitrates converted back to surface nitrates, as was evidenced by the IR spectra. The IR spectrum of a water-exposed, NO_2-saturated BaO/γ-Al_2O_3 sample after annealing to 673 K was identical to that of the NO_2-saturated, H_2O-free sample. In addition, the TPD profile obtained under vacuum conditions, from the water-exposed, NO_2-saturated BaO/γ-Al_2O_3 sample was identical to that recorded without H_2O exposure. These results were rationalized by the fact that H_2O desorbed from the NO_2-saturated sample prior to the onset of surface nitrate decomposition. Therefore, as water was removed from the sample, some of the bulk nitrates converted back to surface nitrates. The TPD experiments we are discussing in the current study, however, were conducted in the presence of H_2O in the He carrier gas. Under these conditions the bulk to surface nitrate re-conversion is delayed due to the presence of water on the surface to much higher temperatures than under vacuum (the presence of water shifts the surface to bulk nitrate equilibrium toward the bulk

Table 2
Summary of the amount of NO_2 and NO released (in %) during the TPD after NO_2 saturation at 523 K on BaO-, SrO-, CaO- and MgO/γ-Al_2O_3

Catalysts	NO_2 (%)		NO (%)	
	~~H_2O~~	H_2O	~~H_2O~~	H_2O
MgO/Al_2O_3	94.2	79.3	5.8	20.7
CaO/Al_2O_3	53.3	52.6	46.7	47.4
SrO/Al_2O_3	45.4	41.6	54.6	58.4
BaO/Al_2O_3	36.4	31.7	63.6	68.3

Comparison between TPD under He flow and TPD under 1% water in He flow.

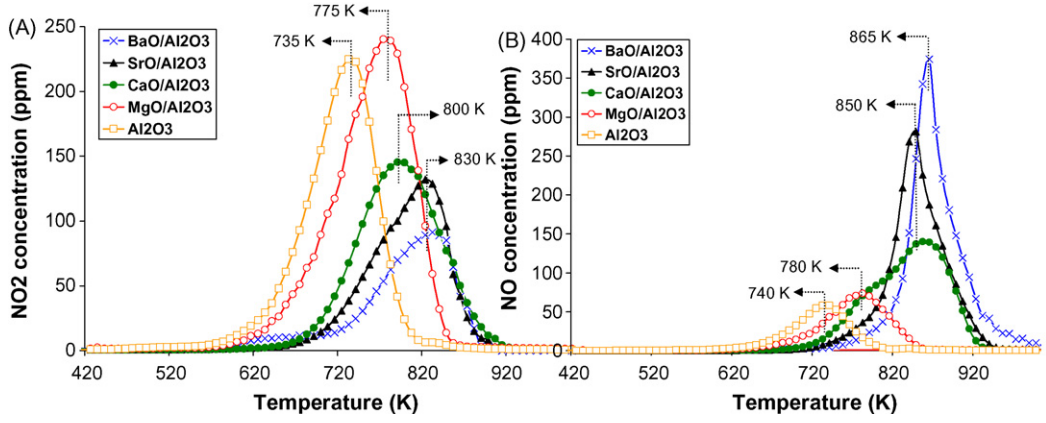

Fig. 5. TPD spectra from BaO-, SrO-, CaO- and MgO/γ-Al_2O_3 under 1% water in He flow after NO_2 saturation at 523 K. NO_2 (A) and NO (B) traces.

side). Therefore, the amount of NO_x desorbing from the bulk nitrates increased, while that from the surface nitrates decreased. The shift in the NO_2 desorption temperature (surface nitrate decomposition) may be well explained just as a simple concentration effect commonly observed in TPD experiments.

The TPD results presented here confirm the same behavior for the other AEO NO_x storage materials. The presence of water induces a modification of the surface-to-bulk nitrate ratio. At the H_2O level applied in this study (1%) part of the surface nitrates is converted into bulk nitrates, and the extent of this phase transformation seems to follow the order of basicity; i.e. the smallest for $CaO/\gamma\text{-}Al_2O_3$ and the largest for $BaO/\gamma\text{-}Al_2O_3$. However, $MgO/\gamma\text{-}Al_2O_3$ shows a slightly different behavior which resembles that of the alumina support, rather than the other alkaline earth oxides, due, most probably, to the loss of Mg during sample preparation, discussed in detail above.

4. Conclusions

The goal of this study was to compare the behavior of $BaO/\gamma\text{-}Al_2O_3$ with other alkaline earth oxides ($SrO/\gamma\text{-}Al_2O_3$, $CaO/\gamma\text{-}Al_2O_3$ and $MgO/\gamma\text{-}Al_2O_3$) during NO_2 uptake and release. The ratio of the two kinds of nitrate species (i.e. surface and bulk nitrates) is strongly correlated with the basicity of the alkaline earth oxide loaded onto the $\gamma\text{-}Al_2O_3$ support; i.e. $BaO/\gamma\text{-}Al_2O_3$, $SrO/\gamma\text{-}Al_2O_3$, $CaO/\gamma\text{-}Al_2O_3$ and $MgO/\gamma\text{-}Al_2O_3$. The amount of bulk nitrate increases with the basicity of the alkaline earth oxide. Consequently, the amount of surface nitrates decreases along this series. The properties of $MgO/\gamma\text{-}Al_2O_3$ in the NO_2 uptake experiments resemble those of the alumina support. The complete absence of bulk $Mg(NO_3)_2$ species after NO_2 exposure indicates that during sample preparation, a significant loss of $Mg(NO_3)_2$ (the precursor) took place. Water has the same effect on each NO_2-saturated alkaline earth oxide: it leads to the decrease of the surface alkaline earth nitrate phase and the concomitant increase of the bulk alkaline earth nitrate phase. These results may have significant implications on the choice of material used in practical NO_x storage applications.

Acknowledgments

Financial support was provided by the U.S. Department of Energy (DOE), office of Freedom Car and Vehicle Technologies. The work was performed in the Environmental Molecular Sciences Laboratory (EMSL) at the Pacific Northwest National Laboratory (PNNL). The EMSL is a national scientific user facility and supported by the U.S. DOE Office of Biological and Environmental Research. PNNL is a multiprogram national laboratory operated for the U.S. DOE by Battelle Memorial Institute under Contract DE-AC06-76RLO 1830.

References

[1] W.S. Epling, L.E. Campbell, A. Yezerets, N.W. Currier, J.E. Parks, Catal. Rev. -Sci. Eng. 46 (2004) 163.
[2] M. Takeuchi, S. Matsumoto, Top. Catal. 28 (2004) 151.
[3] L.J. Gill, P.G. Blakeman, M.V. Twigg, A.P. Walker, Top. Catal. 28 (2004) 157.
[4] H. Mahzoul, J.F. Brilhac, P. Gilot, Appl. Catal. B-Environ. 20 (1999) 47.
[5] J.H. Kwak, D.H. Kim, T. Szailer, C.H.F. Peden, J. Szanyi, Catal. Lett. 111 (2006) 119.
[6] P.J. Schmitz, R.J. Kudla, A.R. Drews, A.E. Chen, C.K. Lowe-Ma, R.W. McCabe, W.F. Schneider, C.T. Goralski, Appl. Catal. B-Environ. 67 (2006) 246.
[7] E. Ozensoy, C.H.F. Peden, J. Szanyi, J. Catal. 243 (2006) 149.
[8] E. Fridell, M. Skoglundh, B. Westerberg, S. Johansson, G. Smedler, J. Catal. 183 (1999) 196.
[9] F. Prinetto, G. Ghiotti, I. Nova, L. Lietti, E. Tronconi, P. Forzatti, J. Phys. Chem. B 105 (2001) 12732.
[10] J. Szanyi, J.H. Kwak, J. Hanson, C.M. Wang, T. Szailer, C.H.F. Peden, J. Phys. Chem. B 109 (2005) 7339.
[11] J. Szanyi, J.H. Kwak, D.H. Kim, S.D. Burton, C.H.F. Peden, J. Phys. Chem. B 109 (2005) 27.
[12] J. Despres, M. Koebel, O. Krocher, M. Elsener, A. Wokaun, Appl. Catal. B-Environ. 43 (2003) 389.
[13] M. Piacentini, M. Maciejewski, A. Baiker, Appl. Catal. B-Environ. 60 (2005) 265.
[14] M. Miletic, J.L. Gland, K.C. Hass, W.F. Schneider, Surf. Sci. 546 (2003) 75.
[15] T. Szailer, J.H. Kwak, D.H. Kim, J. Szanyi, C.M. Wang, C.H.F. Peden, Catal. Today 114 (2006) 86.
[16] E.J. Karlsen, M.A. Nygren, L.G.M. Pettersson, J. Phys. Chem. B 107 (2003) 7795.
[17] M. Piacentini, M. Maciejewski, A. Baiker, Appl. Catal. B-Environ. 59 (2005) 187.
[18] J. Szanyi, J.H. Kwak, D.H. Kim, X.Q. Wang, R. Chimentao, J. Hanson, W.S. Epling, C.H.F. Peden, J. Phys. Chem. C 111 (2007) 4678.
[19] J. Baltrusaitis, J. Schuttlefield, J.H. Jensen, V.H. Grassian, Phys. Chem. Chem. Phys. 9 (2007) 4970.
[20] E. Ozensoy, C.H.F. Peden, J. Szanyi, J. Phys. Chem. B 109 (2005) 15977.
[21] M.H. Brooker, D.E. Irish, G.E. Boyd, J. Chem. Phys. 53 (1970) 1083.
[22] J.H. Kwak, J.Z. Hu, D.H. Kim, J. Szanyi, C.H.F. Peden, J. Catal. 251 (2007) 189.
[23] D.H. Kim, Y.H. Chin, J.H. Kwak, J. Szanyi, C.H.F. Peden, Catal. Lett. 105 (2005) 259.
[24] D.H. Kim, J.H. Kwak, J. Szanyi, S.D. Burton, C.H.F. Peden, Appl. Catal. B-Environ. 72 (2007) 233.
[25] N.W. Cant, M.J. Patterson, Catal. Lett. 85 (2003) 153.
[26] J. Szanyi, J.H. Kwak, D.H. Kim, X. Wang, J. Hanson, R.J. Chimentao, C.H.F. Peden, Chem. Commun. (2007) 984.